

**Manuscript version: Published Version**

The version presented in WRAP is the published version (Version of Record).

**Persistent WRAP URL:**

<http://wrap.warwick.ac.uk/124379>

**How to cite:**

The repository item page linked to above, will contain details on accessing citation guidance from the publisher.

**Copyright and reuse:**

The Warwick Research Archive Portal (WRAP) makes this work by researchers of the University of Warwick available open access under the following conditions.

Copyright © and all moral rights to the version of the paper presented here belong to the individual author(s) and/or other copyright owners. To the extent reasonable and practicable the material made available in WRAP has been checked for eligibility before being made available.

Copies of full items can be used for personal research or study, educational, or not-for-profit purposes without prior permission or charge. Provided that the authors, title and full bibliographic details are credited, a hyperlink and/or URL is given for the original metadata page and the content is not changed in any way.

**Publisher's statement:**

Please refer to the repository item page, publisher's statement section, for further information.

For more information, please contact the WRAP Team at: [wrap@warwick.ac.uk](mailto:wrap@warwick.ac.uk)

# Design and evaluation of pneumatic micropump module for a portable polymerase chain reaction kit

Cite as: AIP Conference Proceedings **2062**, 020049 (2019); <https://doi.org/10.1063/1.5086596>  
Published Online: 25 January 2019

Yudan Whulanza, Taufik Ariesta Hakim, Muhammad S. Utomo, Shabrina Fadhilah, Jerome Charmet, Ridho Irwansyah, Warjito, and Gandjar Kiswanto



View Online



Export Citation

## ARTICLES YOU MAY BE INTERESTED IN

[Ease fabrication of PCR modular chip for portable DNA detection kit](#)

AIP Conference Proceedings **1817**, 040006 (2017); <https://doi.org/10.1063/1.4976791>

[The effect of jet height in air entrainment process of vertical plunging jet with downcomer](#)

AIP Conference Proceedings **2062**, 020023 (2019); <https://doi.org/10.1063/1.5086570>

[The usability of locally-made miniplate and screw compared to the existing imported miniplate and screw](#)

AIP Conference Proceedings **2092**, 020032 (2019); <https://doi.org/10.1063/1.5096700>

**AIP** | Conference Proceedings

Get **30% off** all  
print proceedings!

Enter Promotion Code **PDF30** at checkout



# Design and Evaluation of Pneumatic Micropump Module for a Portable Polymerase Chain Reaction Kit

Yudan Whulanza<sup>1,2, a)</sup>, Taufik Ariesta Hakim<sup>1</sup>, Muhammad S Utomo<sup>2</sup>, Shabrina Fadhillah<sup>2</sup>, Jerome Charmet<sup>3</sup>, Ridho Irwansyah<sup>1</sup>, Warjito<sup>1</sup>, Gandjar Kiswanto<sup>1</sup>

<sup>1</sup>Department of Mechanical Engineering, Faculty of Engineering, Universitas Indonesia, Indonesia

<sup>2</sup>Research Center for Biomedical Engineering, Faculty of Engineering, Universitas Indonesia, Indonesia

<sup>3</sup>Institute of Digital Healthcare, WMG, University of Warwick, United Kingdom

<sup>a)</sup>Corresponding author: yudan@eng.ui.ac.id

**Abstract.** Engineering an active micropump module to integrate in a portable Polymerase Chain Reaction (PCR) is the ultimate goal of this study. This paper investigates the design of pneumatic pumping module to be embedded in a microfluidic system such as PCR kit. A simulation was introduced to verify the design of the pneumatic micropump module to serve the pumping action in the system. Ultimately, the testing showed that the realized micropump module confirmed the functionality of the pump without any leakage and backflow.

## INTRODUCTION

Polymerase Chain Reaction (PCR) is a molecular technology developed by Nobel Laureate Kary Mullis in the 1980s that allows the fast and inexpensive amplification of DNA fragments in-vitro [1]. PCR is largely based on a series of 20-40 repeated thermal cycles of heating and cooling to facilitate DNA replication by enzymatic reaction. In general, PCR involves three repeated cycles: denaturation (around 95 °C), annealing (45-60 °C), and elongation (around 72 °C) to achieve an exponential increase in target DNA.

Previous study by Whulanza et.al [2] has fabricated the serpentine network to be used as PCR module with a comparable solution produced by micromoulding process. The PCR was designed as a modular block to ease the development process. Later, the PCR module altogether with other modules such as pumping module, heating module and its accessories shall be integrated into a complete diagnostic kit [3, 4].

Here, a study on micropump as the actuation source through which a fluid sample (drugs and therapeutic agents) is transferred from a reservoir to the target [5] is initiated. This typical device has application in a drug delivery system, environmental monitoring and homeland security applications such as Micro Total Analysis Systems ( $\mu$ TAS) or Lab-on-a-Chip (LoC) and Point of Care Testing Systems (POCT) [6, 7]. Recently, the application of micropump has also introduced in system with human cells [8] or microorganism [9]. Therefore, precision and accuracy of such micropump system play an essential role.

The latest development of micropump by Jang et.al. showed a simple, inexpensive and disposable system. These results enable us to apply it in a further microfluidic diagnostic kit [10]. A series of micropumps has also been reported for the development of highly integrated, (quasi-)automatically-operated PCR kit [6].

Micropump is an essential components to control and modulate fluid flow in microfluidic networks [11]. The microfluidic module that being developed is made of elastic elastomer polydimethylsiloxane (PDMS). Therefore, we use the deflection ability of the material to create peristaltic movement as pumping method [12]. This peristaltic movement is created by realizing a chamber that generates volume displacement in the microchannel system [13], [14], [15].

This study emphasizes on designing a pneumatic micropump module that will be integrate in our previous PCR module. The micropump will flow the reagent into the PCR stages with closed-loop system so that the cycle can go on as much as desired (figure 1). Ultimately, the pumping method is designed to support the development of a portable diagnostic kit.

## METHODS

### Fabrication of Pump

The fabrication of this micropump consisted of four main steps: mould fabrication, polydimethylsiloxane (PDMS) casting and curing, membrane preparation and product assembling.

### Mould fabrication

An aluminum mould was fabricated by using a milling process. An EMCO VMC 200 Germany, milling machine was used with an accuracy of 1/100 mm. At the beginning of the process, a pump mould was designed in the CAD program, and the milling process was simulated in the CAM program. There are three types of flat-end mill tools that was used. The diameters used here were 4 mm, 2 mm and 1 mm (Seco Tools, Singapore). A machining process parameter was set with a 3500 RPM spindle rate and a 50 pps feed rate.

### PDMS casting and curing

PDMS (Sylgard 184 silicone; Dow Corning, USA) was casted on the mould. The PDMS was mixed with its curing agent at a ratio of 10 to 1. Then, the mould was put on a vacuum chamber to reduce the amount of air trapped in the PDMS during the previous mixing process. A vacuum pump VE115N, (Value, China) was employed for 45 minutes. Afterwards, the mould was heated in a hot chamber for 15 minutes at 140°C and then peeled.

### PDMS membrane preparation

A similar mixture of PDMS was casted onto a spin coater. The spin coater operated for 30 seconds at 2.500 RPM to produce a membrane with a thickness of 50  $\mu\text{m}$ . Moreover, this casted PDMS was placed into an oven for 5 minutes at a temperature of 80°C to be cross-linked further.

### Micropump assembly

Both layers of PDMS were bonded with the membrane in a series of steps. The bonding process was carried out using a Corona SB plasma treater (BlackHole Lab, France) for 30 seconds for each surface, i.e. the top layer and the bottom layer.

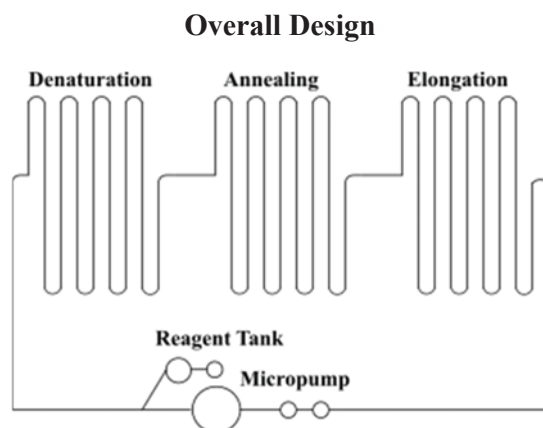


Figure 1. Schematic of PCR-on-a-Chip with micropump to cyclical flow along the PCR path

Figure 1 shows the schematic diagram where the micropump module was utilized in a PCR microfluidic system. Based on previous study by Laser & Santiago [16], a single chamber micropump should strike a flow rate with the average of 20  $\mu\text{L}/\text{min}$ . Provided the dimensions of the channel and the time required for the fluid to flow in each PCR stage (retention time), the velocity of the fluid can be estimated in each stage. Thus, the length of channel required for each stage can be determined corresponded to the velocity of fluid. The length of the channel is formed as serpentine network. Here, it is assumed that the cross section of channel has a perpendicular form with dimension of 300-600  $\mu\text{m}$  wide and 200  $\mu\text{m}$  height. Therefore, the total length of each stage can be determined as shown in table 1.

Table 1. Operational parameter and overall dimension of PCR stages

Stages	Volumetric Flow $Q$ ( $\text{mm}^3/\text{s}$ )	Area of channel $A$ ( $\text{mm}^2$ )	Retention Time $t$ (s)	Length of channel $L$ (mm)
Denaturation	0.33	0.06	30	165
Annealing	0.33	0.06	30	165
Elongation	0.33	0.12	60	165

## Design and Simulation

In order to finalise the design, a set of calculation and numerical simulation were conducted to simulate the pumping mechanism. Initially, each part of the chip and mould are designed by using a Computer Aided Design software ie SolidWorks™. The flow generated by the micropump was numerically simulated by using the COMSOL Multiphysics™. The boundary conditions that were used in the simulation as followed:

Material: PDMS

Density: 970 kg/m<sup>3</sup>

Young's modulus: 750 kPa

Poisson's ratio: 0.45

Physics 1: creeping flow

Boundary 1: inlet - normal inflow velocity – 0.004 m/s

Boundary 2: outlet – pressure – 0 Pa

Boundary 3: wall – no slip

Fluid properties: density – 1000 kg/m<sup>3</sup>; dynamic viscosity – 0.8 Pa.s

Physics 2: solid mechanics

Boundary 1: boundary load – -160 N/m<sup>2</sup> (y-axis)

## Measurement and Testing

### Geometry measurement

The measurement covers the physical dimension of micropump parts such as the diaphragm and the channel for both top and bottom layers. The measurement was done by image analysis using Dinolite digital microscope AM 4113 ZT (Anmo Electronics, Taiwan) at 20x magnification.

### Functional test

The micropump module is tested by flowing water into the inlet channel by using Dolomite peristaltic pump (Dolomite Microfluidics, UK). The flow was set at velocity of 2 mm/s.

### Velocity measurement

The velocity of liquid in the channel is measured using image processing method. The flow of fluid in the channel was captured every second. The distance of fluid was then measured in the image. The velocity was then calculated by dividing the distance traveled by the fluid in every observed time. Here, the observed distance was taken around 20mm from the inlet until outlet channel.

## RESULTS AND DISCUSSION

### Micropump Designs

The pneumatic micropump consists of three layers: the pneumatic channel on the top layer, the thin membrane in the mid layer and liquid fluid channel on the bottom layer (figure 2a). Air will be pumped through the pneumatic channel from the inlet through a pressing mechanism (figure 2b). In the process, the force introduced in the pneumatic channel causes a deformation on its elastic layer thus moves down the thin membrane (figure 2c). The thin membrane acts also as barrier between the air channel and fluid channel in each layer but it delivers the force downward (figure 2d). This deformation act as diaphragm that drives the liquid in the channel in bottom layer. The driven fluid in the liquid channel shall flow in a certain volume corresponded to the delivered pressure onto air channel.

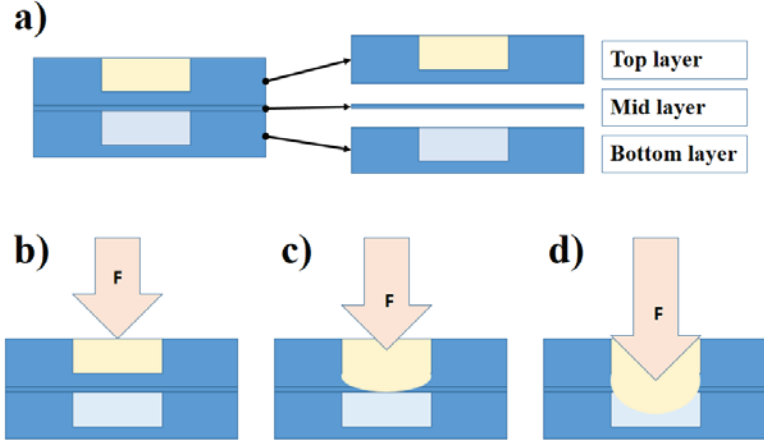


Figure 2. a) The cross section of the micropump module which a sandwich from top layer, mid layer and bottom layer; The pumping mechanics: b) A pneumatic force is introduced on the top layer; c) the elastic top layer moves down and deliver the force downward; d) The cyclic force creates diaphragm movement in the bottom layer thus flow the liquid in the channel.

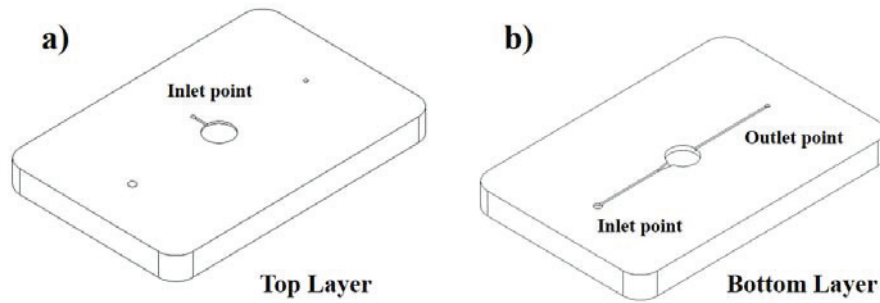


Figure 3. a) Micropump's air channel where air infused in and out to create upward and downward movement; b) Micropump's liquid channel where driven fluid is located

Figure 3a shows that in the air channel, the inlet and outlet is through the same point. During the pumping, air is injected to push the membrane and when the push action is accomplished, the air inside the channel will be sucked back to its initial injection point. The phenomenon results the peristaltic movement of the membrane. The total depth of both liquid and air chip layer is 2.5 mm whereas the depth of the channel is 0.2 mm. The channel width is 0.3 mm, although there is one section in liquid channel where it has larger width (figure 3b). This design is to prevent the backflow phenomenon. With bigger area, liquid tends to flow through to smaller area. Moreover, once the liquid has entered the inlet, it will push the liquid in the channel continuously.

## Simulation Results

The PCR channel design involves all three stages of PCR: denaturation, annealing, and elongation. For denaturation and annealing, the fluid must flow for 30 seconds on each stage, while for elongation it needs 1 minute. The numerical simulation was performed to identify whether the design of the channel will work or not and to obtain the required time of the fluid where at least it needs to flow for 2 minutes from inlet to outlet. .

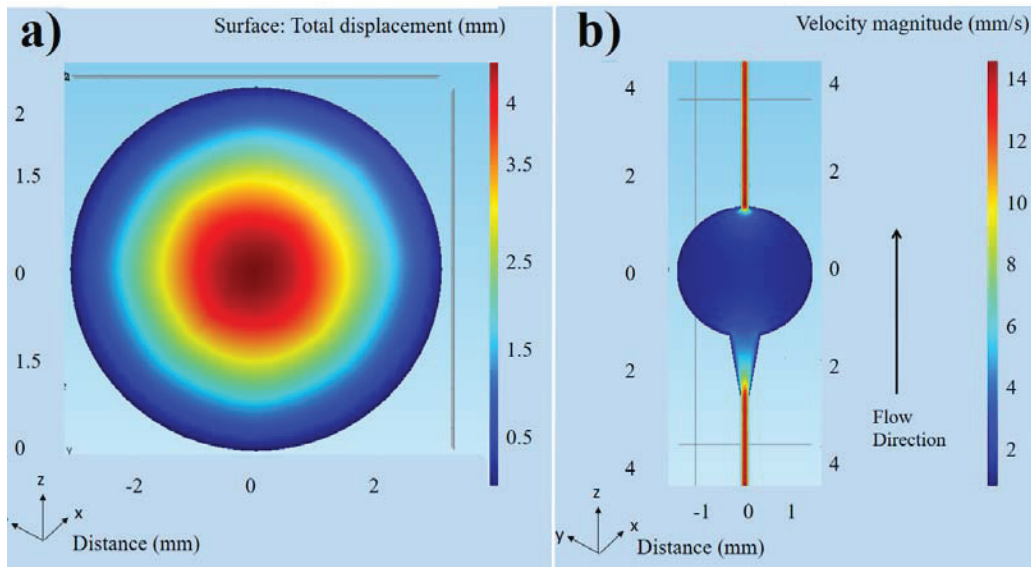


Figure 4. a) Simulation in air channel to observe the displacement trough the membrane when a force is introduced and b) the simulation in the liquid channel to observe velocity distribution throughout the channel during pumping

The velocity magnitude of the channel flow shows a good agreement to that of the calculation result. The velocity in elongation stage is twice slower than the velocity in denaturation stage, and the velocity in annealing is the same as the velocity in denaturation. By applying constant flow rate on the channel will give constant velocity. With the inlet velocity of 5.6 mm/s, the velocity did not decrease until the elongation stage which is 2.76 mm/s.

Figure 4a depicts a deflection of the membrane during pumping action. It shows that most pressure focused on the center of the membrane although the stresses are relatively spread on the side of the membrane. The largest deflection after 0.7 sec of 1.60 kPa pressure applied is 0.5 mm which is deeper than the depth of the channel itself. With that amount of deflection means that the force given during pumping can be arrange to deliver enough pressure to flow fluid in liquid channel. The amount of pressure that resulted is rather different with the simulation from Bui et al that estimate about 5 kPa to deflect the membrane. Whereas, The Chiou group shows that their simulation estimates at pressure of around 3.5 kPa. These differences might be caused by the dimension and the mechanical property of PDMS membrane.

Figure 4b depicts simulation in the liquid channel during pumping. It shows the velocity distribution using the downward force from the air channel. The simulation results that the velocity in the liquid channel gets smaller in the opening of inlet point rather than outlet point. These values are corresponded to the design constraint at the design process. The lower velocity represents a higher pressure in the inlet than the outlet thus the flow goes to outlet direction since it has less resistance.

## Fabrication Results

The realized micropump module is depicted in figure 5. The micropump module has a total dimension of 3 cm long and 2 cm wide in form of an assembled chip (figure 5a). Figure 5b shows the module that breakdown into two chips which are bottom layer and top layer. The graph in table 2 shows the geometry comparison between the mould, the chip and the initial design.



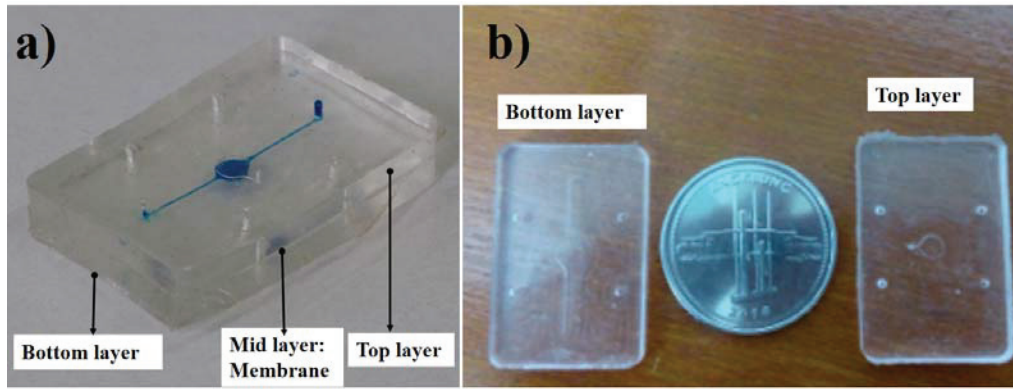


Figure 5. a) Realized module of micropump with coloured fluid inside the liquid channel; b) Breakdown of the micropump module into bottom layer (fluid channel) and top layer (air channel).

Table 2. The measurement of micropump geometry

	Air Diaphragm Radius (mm)	Air Diaphragm Depth (mm)	Liquid Diaphragm Radius (mm)	Liquid Channel Width (mm)	Liquid Channel Depth (mm)
Design	3.00	0.20	3.00	0.30	0.20
Mould	$3.16 \pm 0.03$	$0.20 \pm 0.02$	$3.28 \pm 0.06$	$0.35 \pm 0.07$	$0.26 \pm 0.03$
Product	$2.89 \pm 0.03$	$0.24 \pm 0.07$	$2.89 \pm 0.02$	$0.33 \pm 0.07$	$0.23 \pm 0.01$

Table 2 listed the realized dimension for important feature of the pump such as the diameter and depth of the diaphragm in the air channel. The diaphragm for both in air and liquid channel has a same dimension setting. The realized diaphragm feature has a similar dimension for both in air and liquid part with a margin of 4% from its design. The liquid channel has a rather big margin for its width and depth which were in the range of 10-15% compare to its design. Table 2 also shows that the realized area of channel is 0.076 mm<sup>2</sup> instead of 0.060 mm<sup>2</sup> as designed area.

## Functional Testing

The flow testing has the purpose to test the realized micropump to flow liquid along 20mm distance from a straight channel as depicted in figure 6a. Initially, the liquid was placed in inlet reservoir then pneumatic part was activated with rate of 0.5 stroke/second. The moving liquid was image captured to observe the velocity profile along the channel (figure 6b).

Figure 6b shows an observation of a 14mm length from a total 20mm length of channel. The initial and last part of channel was eliminated. It can be seen that it started with a relatively low velocity at the inlet part. It might indicate a pressure drop near to inlet reservoir. Later, the velocity tends to increase but then drop to a rate similar at the inlet reservoir. This low velocity is caused by the liquid flow through a diaphragm reservoir. However, a sudden increase of flow rate is evident after the liquid exited from the reservoir. Note that the reservoir is where the pressing mechanism took place. At the end of the observation, it can be noted that the velocity tends to decrease. This confirms that the fluid entered the outlet reservoir which has larger area compare to the channel.

A dashed line is also plotted in the figure 6b to compare the velocity from experimental with simulation result in previous section. The simulation however shows an ideal condition of velocity profile in a microfluidic channel. In the simulation environment, the velocity in inlet and outlet were at 12 mm/s and decrease down to 2 mm/s. This decreasing velocity was due to the larger area in pumping reservoir, in which almost similar to the experimental result.

The velocity was then converted to flow rate by multiplying with known area of channel 0.076 mm<sup>2</sup> as measured in table 2. The minimum flowrate is 8.92  $\mu\text{L}/\text{min}$  (0.15 mm<sup>3</sup>/s) whereas the highest is 53.58  $\mu\text{L}/\text{min}$  (0.91 mm<sup>3</sup>/s) as described in figure 6b. These values are in the range of micropump developed by Chiou et al, Jang et al and Pramanick et al. These pumps achieved a flowrate around 5-50  $\mu\text{L}/\text{min}$ .



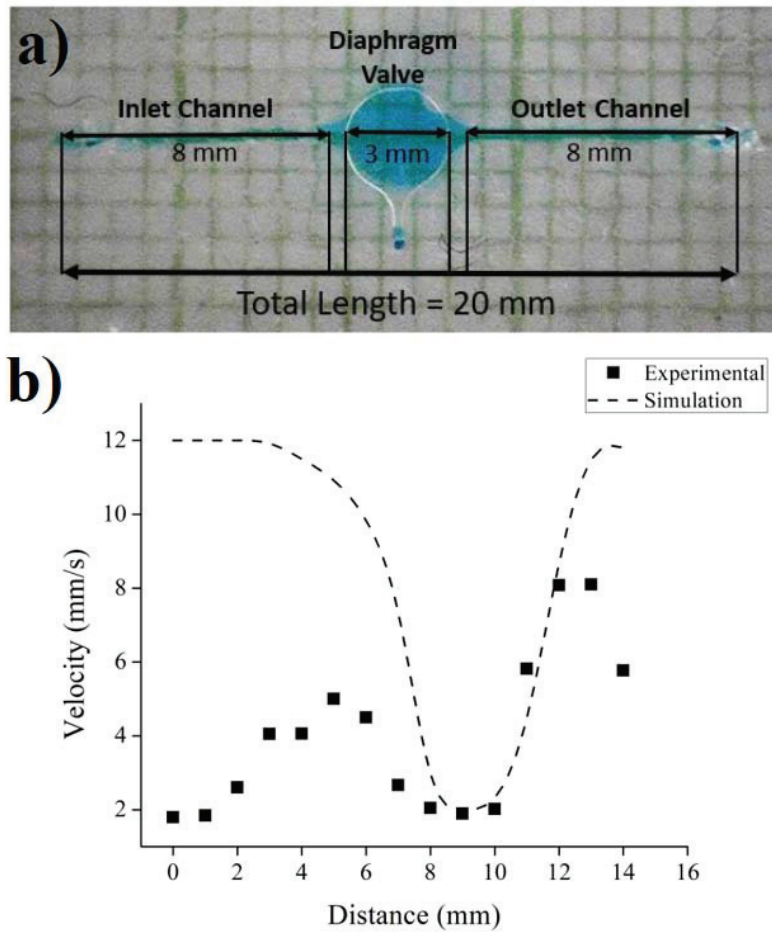


Figure 6. a) The observation of liquid from inlet to outlet point; b) The velocity profile along the traveled path from inlet to outlet point

## CONCLUSION

A PDMS-based pneumatic micropump was designed, manufactured and tested. The numerical simulations gave an information that the pumping mechanism will be occurred at a maximum pressure of 160 Pa and showed a good agreement with the experimental result. The product is realized with a margin around 10% in geometry compare as designed. The function test confirmed to accomplished liquid along 20mm distance.

## ACKNOWLEDGEMENT

This research is funded by Ministry of Research, Technology and Higher Education of Republic of Indonesia in year 2018 under scheme of PDUPT Grant.

## References

- [1] V. Pelt-Verkuil, B. Van and J. P., "A Brief Comparison Between in Vivo DNA Replication and in Vitro PCR Amplification," in *Principles and Technical Aspects of PCR Amplification*, Rotterdam, Springer Netherlands, 2008, pp. 9-15.
- [2] Whulanza, Y., Aditya, R., Arvialido, R., Utomo, M.S and Bachtiar, B.M "Ease Fabrication of PCR Modular Chip for Portable DNA Detection Kit," *AIP Conference Prosiding*, vol. 1817, p. 04006, 2017.
- [3] Phadke, M., Shaner, S., Shah, S., Rodriguez, Y., Wibowo, D., Whulanza, Y., Teriete, P., Allen, J. and Kassegne, S., 2018. Inertial focusing and passive micro-mixing techniques for rare cells capturing microfluidic platform. In *AIP Conference Proceedings*(Vol. 1933, No. 1, p. 040001). AIP Publishing.
- [4] Whulanza, Y., Utomo, M.S. and Hilman, A., 2018. Realization of a passive micromixer using herringbone structure. In *AIP Conference Proceedings* (Vol. 1933, No. 1, p. 040003). AIP Publishing.
- [5] M. Gad-el-Hak, "Journals of Fluid Engineering," *The Fluid Mechanics of Microdevices*, pp. 5-33, 1999.
- [6] P. S. Dittrich, K. Tachikawa and A. Manz, "Micro total analysis systems, latest advancement and trends," in *Analytical Chemistry*, Dortmund, American Chemical Society, 2006, pp. 887-908.
- [7] B. Pramanick, P. K. Dey, S. Das and T. K. Bhattacharyya, "Design and Development of a PDMS Membrane based SU-8 Micropump for drug Delivery System," *Journal of ISSS*, vol. 2, no. 1, pp. 1-9, 2013.
- [8] C. H. Chiou, T. Y. Yeh and J. L. Lin, "Deformation analysis of a pneumatically-activated polydimethylsiloxane (PDMS) membrane and potential micro-pump applications," *Micromachines*, vol. 6, no. 2, pp. 216-229, 2015.
- [9] R. Kant, D. Singh and S. Bhattacharya, "Digitally controlled portable micropump for transport of live micro-organism," *Sensors and Actuators A: Physical*, vol. 265, pp. 138-151, 2017.
- [10] L.-S. Jang, Y.-J. Li, S.-J. Lin, Y.-C. Hsu, W.-S. Yao, M.-C. Tsai and C.-C. Hou, "A stand-alone peristaltic micropump based on piezoelectric actuation," *Biomedical microdevices*, vol. 9, no. 2, pp. 185-194, 2007.
- [11] J. S. Dong, W. H. Chen, P. Zeng, R. G. Liu, C. Shen, W. S. Liu and B. S. Lin, "Design and experimental research on piezoelectric pump with triple vibrators," *Microsystem Technologies*, vol. 23, no. 8, pp. 3019-3026, 2017.
- [12] Y. Yuan, Y. Yalikun, N. Ota and Y. Tanaka, Property Investigation of Replaceable PDMS Membrane as an Actuator in Microfluidic Device, Multidisciplinary Digital Publishing Institute, 2018.
- [13] B. Pečar, D. Križaj, D. Vrtačnik, D. Resnik, T. Dolžan and M. Možek, "Piezoelectric peristaltic micropump with a single actuator," *Journal of Micromechanics and Microengineering*, vol. 24, no. 10, p. 105010, 2014.
- [14] G. T. Bui, J. H. Wang and J. L. Lin, "Optimization of Micropump Performance Utilizing a Single Membrane with an Active Check Valve," *Micromachines*, vol. 9, no. 1, p. 1, 2017.
- [15] J. Xiang, Z. Cai, Y. Zhang and W. Wang, "A micro-cam actuated linear peristaltic pump for microfluidic applications," *Sensors and Actuators A: Physical*, vol. 251, pp. 20-25, 2016.
- [16] D. J. Laser and J. G. Santiago, "A review of Micropumps," *Journal of Micromechanics and Microengineering*, pp. 1-30, 2004.